Study of the ω and ω_3, ρ and ρ_3, and the newly observed ω-like state $X(2220)$

Ya-Rong Wang,[1,2,*] Ting-Yan Li,[1,2,†] Zheng-Yuan Fang,[1,2,‡] Hao Chen,[1,2,3,§] and Cheng-Qun Pang[1,2,3,∥]

[1]*College of Physics and Electronic Information Engineering, Qinghai Normal University, Xining 810000, China*

[2]*Joint Research Center for Physics, Lanzhou University and Qinghai Normal University, Xining 810000, China*

[3]*Lanzhou Center for Theoretical Physics, Key Laboratory of Theoretical Physics of Gansu Province, Lanzhou University, Lanzhou, Gansu 730000, China*

(Received 23 August 2022; accepted 26 October 2022; published 26 December 2022)

We study the excited states of ω and ω_3 by comparison with the ρ and ρ_3 families, and discuss the possibility of $X(2220)$ as ω excitation by analyzing the mass spectra and strong decay behaviors. In addition, we predict the masses and widths of $\omega(2D)$, $\omega_3(4D)$, $\rho_3(4D)$, $\rho_3(1G)$, $\omega_3(2G)$, $\rho_3(2G)$, $\omega_3(3G)$, and $\rho_3(3G)$. The abundant information of their two-body strong decays predicted in this work will be helpful to further study of these ω and ω_3 and ρ and ρ_3 states in experiment and theory.

DOI: 10.1103/PhysRevD.106.114024

I. INTRODUCTION

Very recently, the BESIII Collaboration announced the observation of the $X(2220)$ state in the $e^+e^- \to \omega\pi^0\pi^0$ process [1], which has a statistical significance larger than 5σ. The measurement shows that the $X(2220)$ has the mass of $M = 2222 \pm 7 \pm 2$ MeV and the width of $\Gamma = 59 \pm 30 \pm 6$ MeV. It could be an ω excited state from its report. The Lanzhou group indicates that the enhancement structures around 2.2 GeV existing in $e^+e^- \to \omega\eta$ and $e^+e^- \to \omega\pi^0\pi^0$ contain the $\omega(4S)$ and $\omega(3D)$ signals [2]. The BESIII Collaboration announced $X(2220)$ could be an excited ω resonance [3]. Present studies show that it is reasonable to regard $X(2220)$ as an ω state. When further checking the experimental status of light mesons, we notice an interesting phenomenon: the states of unflavored light meson families with 3^{--} are not established well. In our previous work [4], we carried out a system investigation of the ω mesons and studied the ω-like $X(2240)$ state observed by BESIII Collaboration [5]. Now, we reconsider the newly observed $X(2220)$ state and the ω and ω_3, ρ and ρ_3 families.

*nanoshine@foxmail.com
†litingyan1213@163.com
‡fang1628671420@163.com
§chenhao0602@live.cn
∥Corresponding author.
xuehua45@163.com

As an important part of the meson family, the ω and ρ and ω_3 and ρ_3 families have become more and more abundant in experiment. BESIII Collaboration reported a result that in the $e^+e^- \to \omega\pi^0$ cross section, a resonance denoted by $Y(2040)$ was observed recently. Its mass and width are determined to be $2034 \pm 13 \pm 9$ and $234 \pm 30 \pm 25$ MeV [6], respectively; Ref. [7] also treated it as $\rho(2000)$. BESIII Collaboration also reported a state [we call it $X(2239)$] with the mass of $M = 2239.2 \pm 7.1 \pm 11.3$ MeV and the width of $\Gamma = 139.8 \pm 12.3 \pm 20.6$ MeV [8] by studying the cross section of the $e^+e^- \to K^+K^-$ process. $X(2239)$ is treated as $Y(2175)$ in the Ref. [9]. Reference [4] assigned $X(2239)$ as the $\omega(4^3S_1)$ state and it treated $X(2239)$ as the candidate of tetraquark states in Refs. [10,11]. Barnes, Godfrey, and Swanson suggest that further investigation is expected to understand the structures near the $\Lambda\bar{\Lambda}$ threshold, such as $X(2239)$, $\eta(2225)$, and $X(2175)$. However, the properties of $X(2240)$ still remain unclear [12].

Afonin classified light nonstrange mesons according to the values of (L, n) and indicated that $\omega_3(1670)$, $\omega_3(2285)$, $\rho_3(1690)$, are D-wave mesons [13]. In 2009, Ebert calculated masses of the ground state as well as the orbital and radial excited states of quark-antiquark mesons within the relativistic quark model, which included the masses of ω, ω_3, ρ, and ρ_3 meson families [14]. Anisovish *et al.* consider the decays of ω and ρ mesons, the $^3S_1$ $q\bar{q}$ states of constituent quark model: $\rho \to \gamma\pi$, $\omega \to \gamma\pi$, and $\rho \to \pi\pi$ and give correct values for the partial widths of radiative and hadronic decays of confined $q\bar{q}$ states [15]. In 2013, the Lanzhou group studied the ρ, ρ_3 family [16], which helps to construct the whole ρ family. Later, Wang *et al.* predicted the spectroscopy behavior of ω, ρ, and ϕ mesons at the range of 2.4–3 GeV [17]. Feng *et al.* analyze the masses and two-body strong decay widths of $^3S_1$ vector mesons [18]. The masses and strong decay widths of the higher excited ρ mesons are calculated in Ref. [19]. All of the above mentioned works refer to ω and ω_3 and ρ and ρ_3 mesons.

Not only are the lightest vector meson resonances, ρ, ω, and ϕ benchmark states in understanding of the quark substructure of hadrons [20], but also they are important parts of the light meson family. A systematic study for the ω, ρ, and ω_3, ρ_3 meson family becomes very necessary and urgent. ω and ω_3 and ρ and ρ_3 mesons have same quantum numbers (P and C), for which reason the study of them can be borrowed from each other. We estimate the mass of the missing states in these meson families. Similarly, we study the strong decays of the ω and ω_3 meson family comparing with that of the ρ and ρ_3 meson family.

In this work, we will study the excited states of ω, ρ, and ω_3, ρ_3 mesons. By using the modified Godfrey-Isgur quark (MGI) model and quark pair creation (QPC) model, the mass spectra and strong decay behavior of the excited states of these mesons are analyzed, which indicates that $X(2220)$ is the candidate of $\omega(3D)$ meson with $I(J^P) = 0(1^-)$. The spectra of the ω, ρ and ω_3, ρ_3 meson families are studied.

This paper is organized as follows. We first introduce the models applied in this paper in Sec. II and analyze the mass spectra and decay behaviors of the ω, ρ and ω_3, ρ_3 mesons in Sec. III. The paper ends with a summary.

II. MODELS EMPLOYED IN THE WORK

The modified GI quark model, Regge trajectory, and the QPC model can be used to calculate the mass spectra and the two-body strong decays of the meson family, respectively. Before discussing the results, the above models will be introduced briefly here.

A. Regge trajectory

It is efficient to investigate a light-meson spectrum by determining the Regge trajectory [21,22]. The following relation is satisfied by the masses and radial quantum numbers of the light mesons that belong to the same meson family:

$$M^2 = M_0^2 + (n-1)\mu^2, \tag{2.1}$$

where M_0 represents the mass of the ground state, n is the radial quantum number of the corresponding meson with the mass M, and μ^2 is the trajectory slope. The Regge trajectories are a great method to help us decide the approximate mass range of a particle and it lays a good foundation for our next step. This method can approximately hold even if it is not as strict as the Regge trajectory as a function of the particle spin, it can still approximately hold since at most one or two excitations are known for each quantum number. And we will calculate the mass spectrum using the MGI model, which obviously takes into account spin breaking.

B. The modified GI model

Godfrey and Isgur successfully proposed the GI model in 1985 for characterizing relativistic meson spectra, particularly for low-lying mesons [23]. In order to better describe the spectrum of the highly excited states, Song *et al.* [24,25] introduced the color screening effect on the basis of the Cornell potential to modify the GI model (MGI model).

The Hamiltonian of the potential model reads

$$\tilde{H} = \sqrt{m_1^2 + \mathbf{p}^2} + \sqrt{m_2^2 + \mathbf{p}^2} + \tilde{V}_{\mathrm{eff}}(\mathbf{p}, \mathbf{r}), \tag{2.2}$$

which represents the internal interactions of mesons. m_1 and m_2 are the mass of quark and antiquark, respectively, the effective potential has a familiar format in the nonrelativistic limit before smeared [23,26]

$$V_{\mathrm{eff}}(r) = H^{\mathrm{conf}} + H^{\mathrm{hyp}} + H^{\mathrm{so}}, \tag{2.3}$$

with

$$\begin{aligned} H^{\mathrm{conf}} &= \left[-\frac{3}{4}\left(\frac{b(1-e^{-\mu r})}{\mu} + c\right) + \frac{\alpha_s(r)}{r}\right](\boldsymbol{F}_1 \cdot \boldsymbol{F}_2) \\ &= S(r) + G(r), \end{aligned} \tag{2.4}$$

$$\begin{aligned} H^{\mathrm{hyp}} = -\frac{\alpha_s(r)}{m_1 m_2}\Bigg[&\frac{8\pi}{3}\boldsymbol{S}_1 \cdot \boldsymbol{S}_2 \delta^3(\boldsymbol{r}) \\ &+ \frac{1}{r^3}\left(\frac{3\boldsymbol{S}_1 \cdot \boldsymbol{r}\boldsymbol{S}_2 \cdot \boldsymbol{r}}{r^2} - \boldsymbol{S}_1 \cdot \boldsymbol{S}_2\right)\Bigg](\boldsymbol{F}_1 \cdot \boldsymbol{F}_2), \end{aligned} \tag{2.5}$$

$$H^{\mathrm{so}} = H^{\mathrm{so(cm)}} + H^{\mathrm{so(tp)}}, \tag{2.6}$$

where $\boldsymbol{S}$ indicates the spin of quark or antiquark and $\boldsymbol{L}$ is the orbital momentum. For a meson, $\langle \boldsymbol{F}_1 \cdot \boldsymbol{F}_2 \rangle = -4/3$, the running coupling constant $\alpha_s(r)$ has the following form:

$$\alpha_s(r) = \sum_{k=1}^{3} \frac{2\alpha_k}{\sqrt{\pi}} \int_0^{\gamma_k r} e^{-x^2} dx, \tag{2.7}$$

where $\alpha_{1,2,3} = 0.25,\ 0.15,\ 0.2$ and $\gamma_{1.2.3} = \frac{1}{2}, \frac{\sqrt{10}}{2}, \frac{\sqrt{1000}}{2}$ [23]. H^{conf} reflects the spin-independent interaction, and it can divided into two parts: $S(r)$ and $G(r)$. H^{hyp} represents the color-hyperfine interaction. H^{so} is the spin-orbit interaction that contains the color magnetic term and the Thomas precession term. H^{so} can be written as

$$H^{\mathrm{so(cm)}} = \frac{-\alpha_s(r)}{r^3}\left(\frac{1}{m_1} + \frac{1}{m_2}\right)\left(\frac{\boldsymbol{S}_1}{m_1} + \frac{\boldsymbol{S}_2}{m_2}\right) \cdot \boldsymbol{L}(\boldsymbol{F}_1 \cdot \boldsymbol{F}_2), \tag{2.8}$$

TABLE I. Parameters and their values in this work, which are given by Ref. [27].

Parameter	Value [27]	Parameter	Value [27]
m_u (GeV)	0.163	σ_0 (GeV)	1.799
m_d (GeV)	0.163	s (GeV)	1.497
m_s (GeV)	0.387	μ (GeV)	0.0635
b (GeV^2)	0.221	c (GeV)	−0.240
ϵ_c	−0.138	ϵ_{sov}	0.157
$\epsilon_{\rm sos}$	0.9726	ϵ_t	0.893

$$H^{\rm so(tp)} = -\frac{1}{2r}\frac{\partial H^{\rm conf}}{\partial r}\left(\frac{\boldsymbol{S}_1}{m_1^2}+\frac{\boldsymbol{S}_2}{m_2^2}\right)\cdot \boldsymbol{L}. \qquad (2.9)$$

The parameters of the MGI model are defined in Table I [27].

Through diagonalizing and solving the Hamiltonian in Eq. (2.2) by exploiting a simple harmonic oscillator (SHO) basis, the mass spectra and wave functions can be obtained. The mass and wave function of the meson are applied to the strong decay process.

C. A brief review of QPC model

The QPC model is used to calculate the hadronic strong decays allowed by the Okubo-Zweig-Iizuka (OZI) rule. This model was initially put up by Micu [28] and further developed by the Orsay group [29–33]. The QPC model is widely applied to the OZI-allowed two-body strong decays of mesons in Refs. [16,27,34–56]. The transition operator $\mathcal{T}$ describes a quark-antiquark pair (denoted by indices 3 and 4) creation from vacuum that $J^{PC}=0^{++}$. For the process $A\to B+C$, $\mathcal{T}$ can be written as [4]

$$\mathcal{T} = -3\gamma\sum_m\langle 1m;1-m|00\rangle\int d\mathbf{p}_3 d\mathbf{p}_4\delta^3(\mathbf{p}_3+\mathbf{p}_4) \times\mathcal{Y}_{1m}\left(\frac{\mathbf{p}_3-\mathbf{p}_4}{2}\right)\chi^{34}_{1,-m}\phi^{34}_0(\omega^{34}_0)_{ij}b^\dagger_{3i}(\mathbf{p}_3)d^\dagger_{4j}(\mathbf{p}_4), \qquad (2.10)$$

where $\mathcal{Y}_{\ell m}(\mathbf{p})=|\mathbf{p}|^\ell Y_{\ell m}(\mathbf{p})$ represents the solid harmonics. χ, ϕ, and ω denote the spin, flavor, and color wave functions, respectively. Subindices i and j are the color index of a $q\bar{q}$ pair. The amplitude $\mathcal{M}^{M_{J_A}M_{J_B}M_{J_C}}$ of the decay process is defined with the transition operator $\mathcal{T}$,

$$\langle BC|\mathcal{T}|A\rangle = \delta^3(\mathbf{P}_B+\mathbf{P}_C)\mathcal{M}^{M_{J_A}M_{J_B}M_{J_C}}; \qquad (2.11)$$

$\mathbf{P}$ is the three-momentum in the rest frame of a meson A. Finally, the total width can be expressed in terms of the partial wave amplitude squared,

$$\Gamma = \frac{\pi}{4}\frac{|\mathbf{P}|}{m_A^2}\sum_{J,L}|\mathcal{M}^{JL}(\mathbf{P})|^2, \qquad (2.12)$$

where m_A is the mass of an initial state A, and the two decay amplitudes can be related by the Jacob-Wick formula [57] as

$$\mathcal{M}^{JL}(\mathbf{P}) = \frac{\sqrt{4\pi(2L+1)}}{2J_A+1}\sum_{M_{J_B}M_{J_C}}\langle L0;JM_{J_A}|J_AM_{J_A}\rangle \times\langle J_BM_{J_B};J_CM_{J_C}|J_AM_{J_A}\rangle\mathcal{M}^{M_{J_A}M_{J_B}M_{J_C}}. \qquad (2.13)$$

III. NUMERICAL RESULTS AND PHENOMENOLOGICAL ANALYSIS

We adopt the Regge trajectory and the MGI model to calculate the mass spectrums of ω and ω_3 and ρ and ρ_3 mesons and employ the QPC model with the meson wave functions obtained from the MGI model to evaluate the meson decay widths. Following, we will give the numerical results and phenomenological analysis.

A. Mass spectra analysis

We plot the Regge trajectory of ω and ω_3, ρ and ρ_3 meson families in the Fig. 1. By analyzing the Regge trajectory, the results demonstrate that $\omega(782)$, $\omega(1420)$, and $\omega(1960)$ are $1S$, $2S$, and $3S$ states, respectively. $\rho(770)$, $\rho(1450)$, $\rho(1900)$, and $\rho(2150)$ are $1S$, $2S$, $3S$, and $4S$ states. However, the situation of $\omega(4S)$ is not so distinct. $\omega(2330)$, $\omega(2290)$, and $X(2240)$ can be the candidates of $\omega(4S)$ because of their approximate masses. The widths of those states are different. The mass of $\omega(2330)$ is larger than that of others, more details can be seen in the Fig. 1 and the numerical result in Table II. As for the D wave, the states $\rho(1700)$, $\rho(2000)$, and $\rho(2270)$ are on the $(n+I+J,M^2)$ planes. We assign $X(2220)$ and $\omega(2205)$ as the 3^3D_1 states. $\omega_3(1945)$ and $\omega_3(2285)$ are the excited states of $\omega_3(1670)$. $\rho_3(1990)$ and $\rho_3(2250)$ are the $2D$ and $3D$ states, which agrees well with the results in Ref. [16]. We can see the masses of $\omega(1650)$ and $\rho(1700)$, $\omega_3(1670)$ and $\rho_3(1670)$, $\omega_3(1945)$ and $\rho_3(1990)$ are very similar.

Applying the MGI model and the parameters in Table I, the mass spectra of S wave and D wave of ω and ρ mesons as well as ω_3 and ρ_3 mesons are shown in the Table II. Jia *et al.* revisited the orbital Regge spectra of the light unflavored mesons [58]. And as we reviewed in Sec. I, Anisovich *et al.* investigated the Regge trajectory [59], Ebert *et al.* gave the mass spectrum of the ω and ω_3 and ρ and ρ_3 mesons [14]. Our numerical results are compared with experimental masses and their theoretical results in Table II. As shown in Table II, Ref. [59] estimated the mass of $\omega_3(1D)$ to be 1671 MeV, which is smaller than the mass obtained with the MGI model and Ref. [14]. The mass of $\omega(1^3S_1)$ calculated in the MGI model is smaller than that in Refs. [14,58,59]. The mass spectrum of Ref. [59] and MGI model all indicate that the newly observed state $X(2220)$ may be an $\omega(3D)$ state. Furthermore, we find that the lower

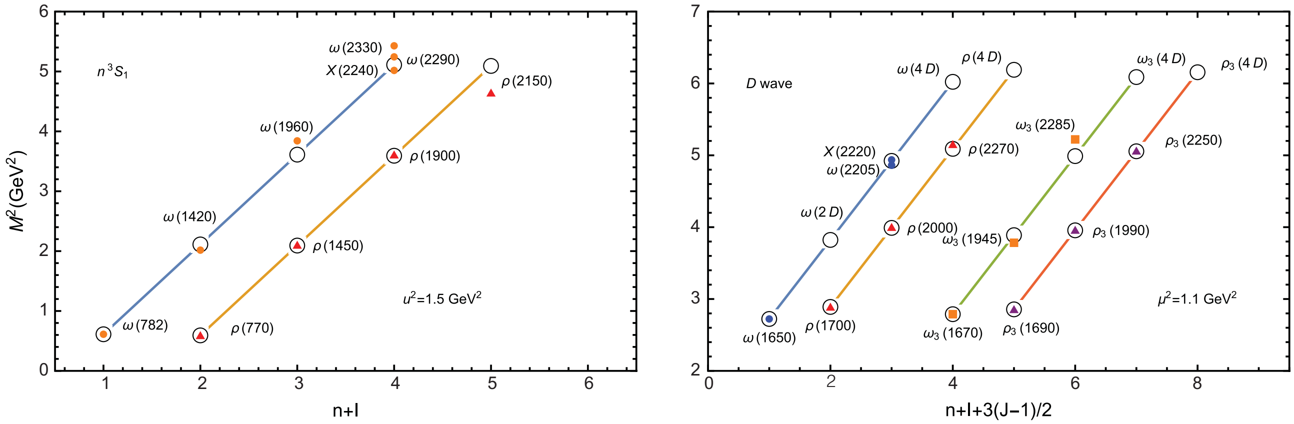

FIG. 1. The S and D waves' Regge trajectories of ω, ω_3 and ρ, ρ_3 families. Here J is the angular momentum of the meson. The open circle and the filled geometry are the theoretical and experimental values, respectively.

TABLE II. The mass spectra of ω and ω_3 and ρ and ρ_3 mesons. The unit is MeV.

$n^{2s+1}L_J$	Jia [58]	Anisovish [59]	Ebert [14]	This work	Experimental mass
$\omega(1^3S_1)$	846	778	776	773.8	782.65 ± 0.12 [60]
$\rho(1^3S_1)$	775				775.26 ± 0.25 [60]
$\omega(2^3S_1)$		1473	1486	1424.3	1410 ± 60 [60]
$\rho(2^3S_1)$					1465 ± 25 [60]
$\omega(3^3S_1)$		1763	1921	1906.1	1960 ± 25 [60]
$\rho(3^3S_1)$					1909 ± 30.2 [61]
$\omega(4^3S_1)$		2158	2195	2259.1	2330 ± 30, [60] 2290 ± 20, [60] $2239.2 \pm 7.1 \pm 11.3$ [8]
$\rho(4^3S_1)$					2201 ± 19 [62]
$\omega(5^3S_1)$		2363		2542.1	⋯
$\rho(5^3S_1)$					⋯
$\omega(1^3D_1)$		1701	1557	1646.2	1670 ± 30 [60]
$\rho(1^3D_1)$					1720 ± 20 [60]
$\omega(2^3D_1)$		1992	1895	2047.6	⋯
$\rho(2^3D_1)$					2000 ± 30 [63]
$\omega(3^3D_1)$		2212	2168	2365.0	2205 ± 30, [60] 2222 ± 7.3 [1]
$\rho(3^3D_1)$					2265 ± 40 [60]
$\omega(4^3D_1)$				2624.0	⋯
$\rho(4^3D_1)$					⋯
$\omega_3(1^3D_3)$	1661	1671	1714	1708.2	1667 ± 4 [60]
$\rho_3(1^3D_3)$	1675				1688.8 ± 2.1 [60]
$\omega_3(2^3D_3)$		1987	2066	2074.0	1945 ± 20 [60]
$\rho_3(2^3D_3)$					1982 ± 14 [60]
$\omega_3(3^3D_3)$		2376	2309	2374.0	2285 ± 60 [60]
$\rho_3(3^3D_3)$					2232 [60]
$\omega_3(4^3D_3)$		2705		2628.8	⋯
$\rho_3(4^3D_3)$					⋯
$\omega_3(1^3G_3)$		2252	2002	2254.8	2255 ± 15 [60]
$\rho_3(1^3G_3)$					⋯
$\omega_3(2^3G_3)$		2482	2267	2522.3	⋯
$\rho_3(2^3G_3)$					⋯
$\omega_3(3^3G_3)$		2746		2748.5	⋯
$\rho_3(3^3G_3)$					⋯

TABLE III. The total and partial decay widths of the $\omega(2S)$ and $\rho(2S)$, the unit of width is MeV. The γ value is 11.5–13.4.

$\omega(1420)$, $\Gamma_{\rm exp} = 880 \pm 170$ [68]			$\rho(1450)$, $\Gamma_{\rm exp} = 400 \pm 60$ [66]		
Channel	Value	Reference [67]	Channel	Value	Reference [67]
Total	690 ± 105	378	Total	400	279
$\pi\rho$	608	328	$\pi\omega$	220	122
$\eta\omega$	33.3		$\eta\rho$	58.0	
KK	28.3	31	KK	31.9	
$b_1\pi$	12.1	1	$\pi\pi$	30.9	74
KK^*	9.50	5	KK^*	30.3	
			$a_1\pi$	14.9	3
			$h_1\pi$	9.05	1

energy excited states such as $1S$, $2S$ and $1D$, $2D$ are consistent with experimental values [60,63].

As for ω_3 and ρ_3 meson families, there is too little information to help us determine their structures. For the states of D wave, $\omega_3(1670)$ and $\rho_3(1690)$ are the $1D$ states which has been certified by many researchers [13,14,64,65]. With respect to $2D$ states, we predict the masses of $\omega(2D)$ and $\rho(2D)$ are both 2074 MeV. At the same time, $\rho(2000)$ is a $\rho(2D)$ state [13,16], which is also close to our theoretical prediction. With regard to the $3D$ states of ω_3 and ρ_3, the value of the mass that we calculated is 2376.5 MeV. Moreover, we consider $\rho_3(2250)$ as the $\rho_3(3D)$ state, which agrees well with the result in Ref. [16].

Besides, we have also calculated the mass spectra of ω_3 and ρ_3 of G wave. The masses of $1G$, $2G$, and $3G$ are 2254.8, 2522.3, and 2748.5 MeV, respectively. Further discussion based on the decay behaviors will be given in the next section. We hope that this information can help find these resonances in experiment.

B. Decay modes and width

ω and ω_3 and ρ and ρ_3 mesons have the same quantum numbers (P and C), for which reason the study of them can be learned from each other. We estimate the masses of the missing states in these meson families. Similarly, we study the strong decays of ω and ω_3 meson family comparing with that of ρ and ρ_3 meson family. The γ value in Eq. (2.10) is taken by the following method. When fitting the ρ and ρ_3 meson experimental width value (with error) using the theoretical total width, the range of γ value can be fixed. Then we use this γ value to calculate the width of ω and ω_3 meson. Some decay channels which less than 1 MeV are omitted.

1. S wave ω and ρ mesons

By analyzing the above masses of ω and ρ states, we know that $\omega(1420)$, $\omega(1960)$, $\omega(2330)$, $\omega(2290)$, and $X(2240)$ are the radial excitations of $\omega(782)$. $\rho(1450)$, $\rho(1900)$, and $\rho(2150)$ are the $\rho(2S)$, $\rho(3S)$, and $\rho(4S)$ states, respectively. We will then discuss these states.

From Table III, $\omega(1420)$ dominantly decay into $\pi\rho$ which is consistent with experiment [66] and Ref. [67]. $\eta\omega$, KK, $b_1\pi$, and KK^* are the important decay modes in which $b_1\pi$ was observed in experiment [66]. The total width of $\omega(1420)$ in our calculation has a overlap with the experiment value [68]. $\omega(1420)$ is a good candidate of $\omega(2S)$ which is consistent with Ref. [51].

$\omega(1960)$ is observed in the $p\bar{p} \to \omega\eta$, and $\omega\pi\pi$ process [69]. As shown in Table IV, $\omega(1960)$ dominantly decay into $\rho\pi$ under $\omega(3S)$ assignment. The decay modes $b_1\pi$, KK_1, and $\eta\omega$ make some contribution to the total width, and $b_1\pi$ can decay to $\omega\pi\pi$ which is the final channel observed in experiment [69]. According to our calculation, the total width of $\omega(1960)$ is 191.1 ± 42.5 MeV and this is consistent with the experimental data [69]. In addition, $\eta\omega$ is a sizable final channel and has been observed in experiment [69]. Other detailed information is demonstrated in Table IV. Our calculation indicates that $\omega(1960)$ can be assigned as $\omega(3S)$ state, which is consistent with Ref. [18].

$X(2240)$ is observed in the $e^+e^- \to K^+K^-$ process by the BESIII Collaboration, which has the mass of $2239.2 \pm 7.1 \pm 11.3$ MeV and the width of $139.8 \pm 12.3 \pm 20.6$ MeV [8]. The quantum number of this resonant structure can be assigned as $J^{PC} = 1^{--}$. Assuming that

TABLE IV. The total and partial decay width of the $\omega(3S)$ and $\rho(3S)$, the unit of width is MeV. The γ value is 6.3–7.9.

$\omega(1960)$, $\Gamma_{\rm exp} = 195 \pm 60$ [69]		$\rho(1900)$, $\Gamma_{\rm exp} = 130 \pm 30$ [67]	
Channel	Value	Channel	Value
Total	191 ± 42.5	Total	130
$\rho\pi$	108	$a_2\pi$	31.1
$b_1\pi$	32.0	$\pi\omega$	29.2
KK_1	14.8	KK_1	18.7
$\eta\omega$	9.90	$\pi\pi(1300)$	16.1
$KK^*(1410)$	9.40	$\pi\pi$	13.9
$h_1\eta$	4.74	$a_1\pi$	13.0
KK^*	3.77	KK	2.60
KK	3.14	$b_1\eta$	2.55
KK_1'	2.35	KK^*	2.46

TABLE V. The total and partial decay widths of the $\omega(4S)$ and $\rho(4S)$, the unit of width is MeV. The γ value is 6.9–11.3.

	$\omega(2330)$	$\omega(2290)$	$X(2240)$	$\rho(2150)$	
Channel	Value	Value	Value	Channel	Value
Γ_{exp}	435 ± 75 [60]	275 ± 35 [60]	139.8 ± 23.99 [8]	Γ_{exp}	310 ± 140 [72]
Total	372 ± 170	346 ± 158	306 ± 140	Total	310
$\pi\rho(1450)$	134	122	95.8	$\pi\omega_3$	58.6
$\pi\rho$	62.6	68.0	69.0	$a_2\pi(1700)$	40.7
$b_1\pi$	61.6	54.4	42.4	$\pi\pi(1300)$	32.1
$a_1\rho$	37.2	39.0	37.3	$\pi\omega$	31.5
$\pi\rho_3$	19.5	17.3	12.9	$a_2\pi$	23.1
KK_1	8.39	8.33	6.69	$h_1\pi$	14.7
$f_1\omega$	7.84	6.28	4.28	$a_1\pi$	13.6
$h_1\eta$	7.01	7.53	7.54	$b_1\rho$	11.5
K^*K^*	5.91	5.65	4.88	$\pi\pi$	11.4
$\eta\omega$	4.81	3.28	1.70	$a_1\omega$	10.5
$KK(1460)$	4.81	3.45	2.00	$\pi\omega$	8.31
$a_2\rho$	2.65	11.5	19.0	$\rho\rho$	7.74
KK	0.599	0.503	0.379	KK_1'	6.47
KK_1'	0.421	0.224	0.0783	$f_2\rho$	6.19
K^*K_1	0.164	0.152	0.0761	$\pi\pi_2$	5.98
$KK^*(1430)$	0.121	0.0366	0.00138	$a_0\omega$	5.49
$f_2\omega$	0.0228	1.39	4.97	$a_2\omega$	5.34
				$f_1\rho$	4.99
				K^*K^*	4.20
				$KK^*(1410)$	2.92
				$b_1\eta$	1.74
				$KK(1460)$	1.20
				$\eta\rho$	0.99
				$\eta\rho(1450)$	0.903

it is a isospin scalar state, it may be a $\omega(4S)$ candidate from our previous mass analysis. The state $X(2240)$ needs more theoretical and experimental research to recover its structure. $\omega(2330)$ is firstly observed in the $\gamma p \to \rho^{\pm}\rho^0\pi^{\mp}$ process [70]. It has the mass of 2330 ± 30 MeV and the width of 435 ± 75 MeV. $\omega(2290)$ is reported in the partial wave analysis of the data on $p\bar{p} \to \bar{\Lambda}\Lambda$ [71], which has the mass of 2290 ± 20 MeV and the width of 275 ± 35 MeV. $\omega(2330)$, $\omega(2290)$, and $X(2240)$ are the candidates of the $\omega(4S)$ according to our calculation and the obtained widths are in good agreement with experimental values. $\pi\rho(1450)$ is the primary decay mode of $\omega(2330)$, $X(2240)$, and $\omega(2290)$ if assign them as $\omega(4S)$ states. Besides, $\pi\rho$, $b_1\pi$, and $a_1\rho$ make needful contribution to the total width of $\omega(4S)$, other decay modes contribute less to the total width as shown in Table V.

As for S wave states of the ρ family, we assign $\rho(1450)$, $\rho(1900)$, and $\rho(2150)$ as $\rho(2S)$, $\rho(3S)$, and $\rho(4S)$ states, which consists with the results of Refs. [13,14,16,17]. When $\rho(1450)$ is treated as the $\rho(2S)$, $\pi\omega$ and $\eta\rho$ are predicted to be its important decay channels. KK, $\pi\pi$, and KK^* are the sizable decay modes as well. $\rho(1900)$ is a good candidate of $\rho(3S)$. As shown in the second column of Table IV, the decay modes of $\rho(1900)$ are predicted. $a_2\pi$, $\pi\omega$, and KK_1 are its important decay modes. $\pi\pi(1300)$, $\pi\pi$, and $a_1\pi$ are the sizable final states, which is consistent with Ref. [73]. We assign $\rho(2150)$ as $\rho(4S)$ based on our calculation. The channels $\pi\omega_3$, $a_2(1700)\pi$, $\pi\pi(1300)$, and $\pi\omega$ are the main channels. Otherwise, $a_2\pi$, $h_1\pi$, $a_1\pi$, and $b_1\rho$ have sizable contributions to the total width of $\rho(4S)$.

2. *D*-wave ω and ρ mesons

In this section, we will give an analysis for the D-wave ω and ρ mesons by the means of their two-body strong decay behaviors.

$\omega(1650)$ is well established as a $1D$ state in the ω family in theory [4,51,66], and its dominant decay channel is $b_1\pi$, whose branching ratio is about 0.8. $\pi\rho$, KK, $\eta\omega$, and KK^* are the important modes. $\rho(1700)$ is a good candidate of the 1^3D_1 ρ meson. The analysis of $\rho(1700) \to 2\pi, 4\pi$ [74] and the study of $e^+e^- \to \omega\pi$ via the nonrelativistic $^3P_0$ quark model [75] both indicate that $\rho(1700)$ is a 1^3D_1 state. $\rho(1700)$ mainly decays into $a_1\pi$, $h_1\pi$, and $\rho\rho$ with branching ratios being about 0.38, 0.34, and 0.11, respectively. More information can be seen in Table VI.

As is shown in Fig. 1 and Table II, the mass of $\omega(2D)$ is predicted, which is still unobserved. $\omega(2D)$ has the total width of about 212 ± 36.1 MeV. $b_1\pi$ is its dominant decay

TABLE VI. The partial decay widths of the $\omega(1D)$, $\rho(1D)$, the unit of width is MeV. The γ value is 4.14–6.3.

$\omega(1650)$, $\Gamma_{\text{exp}} = 315 \pm 35$ [66]			$\rho(1700)$, $\Gamma_{\text{exp}} = 250 \pm 100$ [66]		
Channel	Value	Reference [67]	Channel	Value	Reference [67]
Total	284 ± 113	542	Total	250	435
$b_1\pi$	272	371	$a_1\pi$	93.9	134
$\pi\rho$	42.1	101	$h_1\pi$	85.2	124
KK	9.00	35	$\rho\rho$	26.4	14
$\eta\omega$	7.84		$\pi\omega$	14.1	35
KK^*	5.29	21	KK	9.84	36
			$\eta\rho$	8.76	
			KK^*	6.69	
			$a_2\pi$	2.64	

TABLE VII. The total and partial decay widths of the $\omega(2D)$ and $\rho(2D)$, the unit of width is MeV. The γ value is 5.4–6.4.

$\omega(2D)$		$\rho(2000)$, $\Gamma = 260 \pm 45$ [67]	
Channel	Value	Channel	Value
Total	212 ± 36.1	Total	260
$b_1\pi$	110	$a_1(1640)\pi$	58.4
$\pi\rho(1450)$	24.7	$h_1\pi$	36.6
$\pi\rho$	22.7	$\rho\rho$	35.2
$a_1\rho$	22.1	$\pi\pi_2$	34.1
$h_1\eta$	13.2	$a_1\pi$	26.3
$KK^*(1410)$	4.29	$\pi\pi$	21.9
$\eta\omega(1420)$	3.26	$\pi\pi(1300)$	19.8
$\eta\omega$	2.60	$\pi\omega(1420)$	8.22
KK	2.18	$\pi\omega$	6.39
KK_1	1.83	$b_1\eta$	4.50
KK^*	1.15	$KK^*(1410)$	2.54
		KK	1.81
		$\eta\rho$	1.70

channel, whose branching ratio is 0.5. $\pi\rho(1450)$, $\pi\rho$, and $a_1\rho$ are its important decay channels and more details can be seen in Table VII. We suggest that experimentalists focus on these final channels. In 1994, a resonance around 1988 MeV was found in $\bar{p}p \to \pi\pi$ from 0.36 to 2.5 GeV reaction [76]. Later in 2011, Anisovich *et al.* found a resonance that $J^{PC} = 1^{--}$ and its mass is of 2000 ± 30 MeV [77]. $\rho(2000)$ is treated as $\rho(2D)$ state [16,73]. $a_1(1640)\pi$, $h_1\pi$, $\rho\rho$, and $\pi\pi_2(1670)$ have sizable contributions to the total width of $\rho(2D)$.

$X(2220)$ state is found in the $e^+e^- \to \omega\pi^0\pi^0$ process [1], which has the mass of $M = 2222 \pm 7 \pm 2$ MeV and the width of $\Gamma = 59 \pm 30 \pm 6$ MeV. $X(2220)$ is an excellent candidate of $\omega(3D)$ by Regge trajectory analysis and according to Table VIII. When $X(2220)$ is treated as the $\omega(3D)$ state, its width is close to the experiment value. $\omega(2205)$ is also assigned as $\omega(3D)$ state based on mass spectra analysis. $b_1\pi$ is the main decay mode of $\omega(3D)$. $\pi\rho(1450)$ and $a_1\rho$ are the important decay channels of $\omega(3D)$, other modes like $a_2\rho$, $\pi\rho$, and $\pi\rho_3$, and so on also

TABLE VIII. The partial decay widths of the $\omega(3D)$, $\rho(3D)$, Γ_{exp} means the experimental total width, the unit of width is MeV. The γ value is 11.3–14.6.

	$\omega(2205)$	$X(2220)$	$\rho(2270)$	
Channel	Value	Value	Channel	Value
Γ_{exp}	350 ± 90 [60]	59 ± 30.6 [1]	Γ_{exp}	325 ± 80 [69]
Total	147 ± 36.1	164 ± 40.4	Total	325
$b_1\pi$	56.7	66.0	$a_2\omega$	67.0
$\pi\rho(1450)$	21.0	23.7	$\pi\pi(1300)$	64.3
$a_1\rho$	23.7	22.0	$h_1\pi$	42.2
$a_2\rho$	9.08	12.2	$\pi\pi$	39.4
$\pi\rho$	8.32	9.78	$a_1\pi$	26.1
$\pi\rho_3$	6.09	6.97	$\pi\pi_2$	23.2
$f_2\omega$	5.20	6.59	$\rho\rho$	19.5
$f_1\omega$	5.24	5.54	$f_2\rho$	12.0
KK_1	4.78	4.58	$a_1\omega$	5.81
$\pi\rho(1700)$	2.65	2.90	$f_1\rho$	5.67
$h_1\eta$	2.49	3.41	$\omega\pi$	4.51
$\pi(1300)\rho$	1.34	0.495	KK_1	4.00
			$\rho\rho(1450)$	4.00
			$\pi\omega_3$	3.41
			$b_1\eta$	2.58
			$\pi\omega(1650)$	1.5

have contribution to the total width of $\omega(3D)$. We assign $\rho(2270)$ as $\rho(3D)$ state, which is consistent with Ref. [16]. $\rho(2270)$ primarily decays into $a_2\omega$, $\pi\pi(1300)$, and $h_1\pi$. More details can be seen in Table VIII.

3. D-wave ω_3 and ρ_3 mesons

Referring to Particle Data Group (PDG), we can find some experimental results about ω_3 and ρ_3, which are $\rho_3(1690)$, $\rho_3(1990)$, $\rho_3(2250)$, $\omega_3(1670)$, $\omega_3(1945)$, $\omega_3(2285)$, and $\omega_3(2255)$. We carry out an investigation of the Okubo-Zweig-Iizuka allowed a two-body strong decay of the D-wave and G-wave ω_3 and ρ_3 mesons.

There exists a lot of data for $\omega_3(1670)$ from PDG. Amelin *et al.* first found it in the $\pi^-p \to \pi^+\pi^-\pi^0 n$ reactions, which has the mass of $1665.3 \pm 5.2 \pm 4.5$ MeV [78]. And then

TABLE IX. The partial decay widths of the $\omega_3(1D)$, $\rho_3(1D)$, the unit of width is MeV. The γ value is 7.5–9.2.

$\omega_3(1670), \Gamma_{\rm exp} = 90 \pm 20$ [80]		$\rho_3(1690), \Gamma_{\rm exp} = 190 \pm 40$ [60]	
Channel	Value	Channel	Value
Total	81.8 ± 16.5	Total	190
$\pi\rho$	62.8	$\rho\rho$	105
$b_1\pi$	14.7	$\pi\pi$	32.0
$\eta\omega$	2.76	$\pi\omega$	23.1
KK	1.16	πh_1	10.6
		$a_2\pi$	8.07
		$\eta\rho$	3.68
		$a_1\pi$	3.26
		KK	2.66

Baltay *et al.* reported the existence of a high-mass, $I = 0$ resonant state with odd G parity, whose mass and width are $M = 1.63 \pm 0.012$ GeV and $\Gamma = 0.173 \pm 0.016$ GeV [79], respectively. At present, $\omega_3(1670)$ is well established to be a 1^3D_3 state [64]. $\pi\rho$ is the dominant decay mode of $\omega_3(1D)$, which has the branching ratios of 0.77. Additionally, $b_1\pi$, $\eta\omega$, and KK also make contribution to the total width of $\omega_3(1D)$. $\rho_3(1690)$ is well established to be a 1^3D_3 state, which decays into $\rho\rho$, $\pi\pi$, $\pi\omega$, and πh_1 as shown in Table IX and the branching ratios are about 0.55, 0.17, 0.12, and 0.056, respectively. These results are in good agreement with that in Ref. [16].

$\omega_3(1945)$ was firstly observed in the $p\bar{p} \to \omega\eta, \omega\pi^0\pi^0$ [81]. It has the mass of 1945 ± 20 MeV and the width of 115 ± 22 MeV. We assign it as $\omega_3(2D)$ state and calculated the two-body strong decay as shown in Table X. We see from Table X that $b_1\pi$, $\pi\rho$, $\pi\rho(1450)$, and $\pi\rho_3$ are major decay modes of $\omega_3(2D)$. $\eta\omega$, $h_1\eta$, K^*K^*, and KK^* are important channels. When treated as $\rho_3(2D)$, $\rho_3(1990)$ mainly decay into $\pi\pi(1300)$, $a_2\pi$, $\rho\rho$, which branching ratios are 0.22, 0.18, and 0.14, respectively, and this result was certified in Ref. [16]. Besides, $\rho_3(1990) \to \pi a_1, \pi h_1$, $\pi\omega(1420)$ are sizable. More details can be seen in Table IX.

TABLE X. The partial decay widths of the $\omega_3(2D)$, $\rho_3(2D)$, the unit of width is MeV. The γ value is 10.4–11.8.

$\omega_3(1945), \Gamma_{\rm exp} = 115 \pm 22$ [60]		$\rho_3(1990), \Gamma_{\rm exp} = 188 \pm 24$ [69]	
Channel	Value	Channel	Value
Total	105 ± 13.2	Total	188
$b_1\pi$	38.5	$\pi\pi(1300)$	40.6
$\pi\rho$	22.1	$a_2\pi$	34.2
$\pi\rho(1450)$	18.7	$\rho\rho$	26.9
$\pi\rho_3$	11.5	$a_1\pi$	16.7
$\eta\omega$	4.51	$h_1\pi$	16.4
$h_1\eta$	4.44	$\pi\omega(1420)$	15.5
K^*K^*	2.31	$\pi\pi_2$	9.19
KK^*	1.28	$\pi\omega_3$	7.80
		$\pi\omega$	7.14
		$\eta\rho$	4.58
		$b_1\eta$	2.63
		K^*K^*	2.54
		KK^*	1.61

TABLE XI. The partial decay widths of the $\omega_3(3D)$, $\rho_3(3D)$, the unit of width is MeV. The γ value is 6.7–12.5.

$\omega_3(2285), \Gamma_{\rm exp} = 224 \pm 50$ [71]		$\rho_3(2250), \Gamma_{\rm exp} = 135 \pm 75$ [82]	
Channel	Value	Channel	Value
Total	226 ± 126	Total	135
$a_2\rho$	76.3	$a_2\omega$	58.5
$\pi\rho$	32.6	$f_2\rho$	33.7
$f_2\omega$	25.6	$\pi\omega$	12.3
$b_1\pi$	24.5	$\rho\rho$	11.6
$\pi\rho_3$	12.9	$h_1\pi$	11.0
$\pi(1300)\rho$	10.8	$a_2\pi$	9.26
$\pi\rho(1450)$	5.22	$a_1\pi$	8.60
$a_1\rho$	4.37	$\pi\omega_3$	4.32
$\eta\omega$	3.78	$\pi\pi$	3.68
$\eta\omega(1420)$	3.68	$\pi\pi_2$	2.95
$h_1\eta$	3.28	$\pi\omega(1420)$	2.70
$\eta(1295)\omega$	2.14	$b_1\eta$	2.09
K^*K^*	1.45	$KK^*(1410)$	2.06
		$a_1\omega$	1.92
		$\eta\rho$	1.82
		$\eta(1295)\rho$	1.81
		$\eta\rho(1450)$	1.70
		K^*K^*	1.69

As for $\omega_3(3D)$, we consider $\omega_3(2285)$ is the best candidate according to the mass spectra analysis and we give its decay modes and values in Table XI. The total width of $\omega_3(2285)$ is 226 ± 126 MeV if we treat $\omega_3(2285)$ as a $\omega_3(3D)$ state, which is in great agreement with the experimental width [71]. $a_2\rho$, $\pi\rho$, $f_2\omega$, and $b_1\pi$ make great contribution to its total width and $\pi\rho_3$, $\pi(1300)\rho$, $\pi\rho(1450)$, and so forth are also important decay channels. Meanwhile, $\rho_3(2250)$ is established to be a $\rho_3(3D)$ state, which can decay into $a_2\omega$, $f_2\rho$, $\pi\omega$, $\rho\rho$ as shown in Table XI.

$\omega_3(4D)$ and $\rho_3(4D)$ are still missing in experiment. We calculated the width of $\omega_3(4D)$ to be about 290 MeV and $\rho_3(4D)$ is approximately 420 MeV. According to Table XII, the main decay modes of $\omega_3(4D)$ are $a_2\rho$, $\pi(1300)\rho$, $b_1\pi$, and $\pi\rho$. $\rho_3(4D)$ mainly decay into $a_4(2040)\pi$, $a_2(1700)\omega$, $a_2(1700)\pi$, and so on. These predictions can help us search for $\omega_3(4D)$ and $\rho_3(4D)$ states.

4. G-wave ρ_3 and ω_3 mesons

$\omega_3(2285)$ is regarded as $\omega_3(1G)$ in Ref. [13]. The Ref. [69] observed $\omega_3(2255)$ and assigned it as $\omega_3(1G)$ state. According to the mass spectra analysis and two-body decay modes, we agree that $\omega_3(2255)$ may be $\omega_3(1G)$ state. According to Table XIII, $b_1\pi$, $\pi\rho_3$, and $h_1\eta$ are predicted to be $\omega_3(1G)$'s important decay channels, which have the branching ratios of 0.45, 0.14, and 0.1, respectively.

TABLE XII. The partial decay widths of the $\omega_3(4D)$, $\rho_3(4D)$, the unit of width is MeV. The γ value is 11.6.

$\omega_3(2630)$		$\rho_3(2630)$	
Channel	Value	Channel	Value
Total	288	Total	420
$a_2\rho$	57.2	$a_4(2040)\pi$	184
$\pi(1300)\rho$	40.3	$a_2(1700)\omega$	38.7
$b_1\pi$	37.3	$a_2(1700)\pi$	35.4
$\pi\rho$	33.3	$a_2\pi$	25.3
$\pi\rho(1450)$	32.8	$\rho\rho(1450)$	22.4
$\pi\rho_3$	23.0	$f_2\rho$	16.9
$f_2\omega$	17.2	$h_1\pi$	14.3
$\eta(1295)\omega$	8.03	$b_1\rho$	11.8
$\pi_2\rho$	6.85	$\pi\omega(1420)$	10.2
$\eta\omega(1420)$	6.42	$\pi\omega_3$	8.75
$K^*K^*(1410)$	5.65	$\rho\rho$	6.76
$h_1\eta$	5.30	$\pi\pi_2$	6.65
$\eta\omega$	3.46	$K^*K^*(1410)$	5.65
$K^*K_2^*$	2.36	$\eta\rho(1450)$	5.51
f_2h_1	1.94	$\pi\pi$	4.79
$\eta_2\omega$	1.86	$b_1\eta$	4.01
$f_1\omega$	1.66	$a_1\omega$	3.27
a_2b_1	1.50	$K^*K_2^*$	2.36
f_1h_1	1.09	$\pi_2\omega$	2.14
$\pi\rho(1700)$	1.01	h_1a_1	1.94
		b_1b_1	1.83
		$KK^*(1410)$	1.71
		a_2h_1	1.51
		$\eta'\rho(1450)$	1.39
		$\pi\pi(1300)$	1.21
		$h_1\pi(1300)$	1.04

TABLE XIII. The partial decay widths of the $\omega_3(1G)$, $\rho_3(1G)$, the unit of width is MeV. The γ value is 11.6.

$\omega_3(2255)$, $\Gamma_{\rm exp} = 175 \pm 30$ [60]		$\rho_3(2255)$	
Channel	Value	Channel	Value
Total	325	Total	721
$b_1\pi$	147	$\pi\pi_2$	296
$\pi\rho_3$	47.0	$b_1\rho$	76.5
$h_1\eta$	32.9	$\rho\rho$	62.6
$a_2\rho$	23.2	$a_1\pi$	57.4
$\rho\pi$	17.4	$h_1\pi$	46.2
KK_1'	12.5	$a_2\pi$	37.1
$f_2\omega$	11.3	$b_1\eta$	31.5
$\pi\rho(1450)$	8.69	$a_1\omega$	28.9
$\pi(1300)\rho$	5.32	$\pi\omega_3$	16.6
$\eta\omega$	4.00	$\pi\pi(1300)$	14.2
$\pi\rho(1700)$	2.57	$f_2\rho$	12.2
KK_1	2.53	KK_1'	11.7
KK_2^*	2.20	$\pi\omega$	5.86
$\eta'\omega$	1.75	$a_2(1700)\pi$	5.02
$a_1\rho$	1.75	$\omega(1420)\pi$	3.01
$\eta\omega_3$	1.52	$\pi\pi$	2.90
$\eta\omega(1420)$	1.05	KK_1	2.82
$\eta(1295)\omega$	1.04	KK_2^*	2.20
KK^*	1.03	$f_1\rho$	2.201
		$\eta'\rho$	1.87
		$\pi\omega(1650)$	1.54
		$b_1\eta'$	1.27
		$\eta(1295)\rho$	1.15
		KK^*	1.03

We suggest that experimentalists focus on these final channels. The total width of $\omega_3(1G)$ is 325 MeV. The total width of $\rho_3(1G)$ is approximately 721 MeV. $\pi\pi_2$, $b_1\rho$, $\rho\rho$, and $a_1\pi$ are its important decay channels. Considering the final decay channels, $\pi\pi_2$ will be the most important final channels in searching for $\rho_3(1G)$ state experimentally. More details can be seen in Table XIII. These predictions can help us search for and establish $\omega_3(1G)$ and $\rho_3(1G)$ state.

$\omega_3(2G)$, $\rho_3(2G)$, $\omega_3(3G)$, and $\rho_3(3G)$ are still missing, We make predictions about their widths and decay modes. The decay information of the $\omega_3(2G)$ and $\rho_3(2G)$ is listed in Table XIV. As shown in the first column of Table XIV, the strong decay of $\omega_3(2G)$ is predicted, which is still unobserved. $\omega_3(2G)$ has the total width of 312 MeV. $b_1\pi$ is its dominant decay channel, with branching ratio 0.34. $a_2\rho$, $\pi_2\rho$, $\pi\rho_3$, $h_1\eta$, and $\pi\rho$ are the important final states. $\eta'\omega$, $a_1\rho$, and $h_1\eta'$ are small. The total width of $\rho_3(2G)$ is 397 MeV. $\rho_3(2G) \to \pi\pi_2$ will be the dominant decay mode. In the calculation, $h_1\pi$, $a_1\pi$, and $\rho\rho(1450)$ are the important decay channels. Other decay information can be seen in Table XIV.

The decay information of the $\omega_3(3G)$ and $\rho_3(3G)$ are also predicted in this work in Table XV. The total width of $\omega_3(3G)$ is approximately 181 MeV. The channels $b_1\pi$, $\pi\rho$, $\pi\rho_3$, and $f_1\omega$ have the branching ratios of 0.35, 0.07, 0.07, and 0.06, respectively, which are the main decay modes. $\pi_2\rho$, $h_1\eta$, $b_1\pi(1300)$, and $f_2\omega$ are its important decay channels. This work suggests that experimentlists should search for this missing state in $b_1\pi$ final state. Otherwise, $\pi(1300)\rho$, $a_2\rho$, $\pi\rho(1450)$, $a_0\rho$, and $h_1\eta(1295)$ have sizable contributions to the total width of $\omega_3(3G)$. $\rho_3(3G)$ has the total width of about 270 MeV from our calculation. The main decay modes are $\pi\pi_2$, $\rho\rho$, $h_1\pi$, $a_1\omega$, and $a_1\pi$, which branching ratios are 0.17, 0.090, 0.089, 0.086, and 0.078. $a_2\pi$, $a_2(1700)\pi$, $f_2\rho$, $\eta(1295)\rho$, and $\rho\rho(1450)$ are the important decay modes of $\rho_3(3G)$.

IV. CONCLUSION

In this work, we have systematically studied the mass spectra and the OZI-allowed two-body strong decay behaviors of the newly observed $X(2220)$ state as well as ω and ω_3 and ρ and ρ_3 states. We adopt a new way to get the value of γ in ω and ω_3 system. Following is the main work.

(1) The newly observed state $X(2220)$ should be a 3^3D_1 ω state.

(2) The $\omega(782)$, $\omega(1420)$, and $\omega(1960)$ states can be interpreted as the $\omega(1^3S_1)$, $\omega(2^3S_1)$, and $\omega(3^3S_1)$.

TABLE XIV. The partial decay widths of the $\omega_3(2G)$, $\rho_3(2G)$, the unit of width is MeV. The γ value is 11.6.

$\omega_3(2520)$		$\rho_3(2520)$	
Channel	Value	Channel	Value
Total	312	Total	397
$b_1\pi$	107	$\pi\pi_2$	107
$a_2\rho$	40.9	$h_1\pi$	37.1
$\pi_2\rho$	21.4	$a_1\pi$	36.0
$\pi\rho_3$	19.4	$\rho\rho(1450)$	31.4
$h_1\eta$	18.9	$a_1\omega$	22.6
$\pi\rho$	18.6	$b_1\rho$	21.0
$f_2\omega$	17.5	$f_2\rho$	18.4
KK_2	15.3	$b_1\eta$	16.4
$f_1\omega$	13.2	$a_2(1700)\pi$	16.4
$a_0\rho$	9.88	$a_2\pi$	16.04
$\pi(1300)\rho$	4.88	$\rho\rho$	9.21
$\eta_2\omega$	3.57	$\pi_2\omega$	7.03
f_1h_1	3.03	$\pi\omega_3$	6.81
$h_1\eta(1295)$	3.16	b_1b_1	6.46
f_2h_1	3.11	$a_4(2040)\pi$	6.16
$\eta\omega$	3.08	$\pi\pi$	6.15
$f_1(1420)\omega$	3.03	$f_1\rho$	4.72
$h_1\eta'$	2.63	$h_1\pi(1300)$	4.35
$\eta\omega_3$	1.81	KK_2^*	3.81
$a_1\rho$	1.31	$a_2\omega$	3.50
$\eta'\omega$	1.06	$f_1(1420)\rho$	3.20
		ωa_0	3.08
		h_1a_1	2.52
		a_2h_1	2.18
		$\eta\rho_3$	1.50
		$KK(1630)$	1.42
		$\pi\pi(1300)$	1.38
		$b_1\eta'$	1.31

$\omega(2240)$, $\omega(2330)$, and $\omega(2290)$ can be the candidates of $\omega(4^3S_1)$. $\rho(1450)$, $\rho(1900)$, and $\rho(2150)$ are the first, second, and third excited states of $\rho(770)$ as shown in Fig. 1.

(3) The mass and width of $\omega(2D)$, by our prediction, are 2047.6 and 212 ± 36.1 MeV. $\omega(2205)$ and $X(2220)$ are the $\omega(3D)$ states.

(4) $\omega_3(1945)$, $\omega_3(2285)$, and $\rho_3(1990)$, $\rho_3(2250)$ are the first and second excited states of $\omega_3(1670)$ and $\rho_3(1690)$.

(5) The masses of $\omega_3(4D)$ and $\rho_3(4D)$ are both predicted to be 2.63 GeV, the width of them are 288 and 420 MeV. We also predict the mass spectra and decay behaviors of $\omega_3(1G)$ and $\rho_3(1G)$, $\omega_3(2G)$ and $\rho_3(2G)$, and $\omega_3(3G)$ and $\rho_3(3G)$.

TABLE XV. The partial decay widths of the $\omega_3(3G)$, $\rho_3(3G)$, the unit of width is MeV. The γ value is 11.6.

$\omega_3(2750)$		$\rho_3(2750)$	
Channel	Value	Channel	Value
Total	181	Total	270
$b_1\pi$	63.8	$\pi\pi_2$	46.0
$\pi\rho$	12.3	$\rho\rho$	24.3
$\pi\rho_3$	12.0	$h_1\pi$	24.0
$f_1\omega$	11.7	$a_1\omega$	23.6
$\pi_2\rho$	10.4	$a_1\pi$	21.0
$h_1\eta$	9.84	$a_2\pi$	10.5
$b_1\pi(1300)$	8.28	$a_2(1700)\pi$	9.40
$f_2\omega$	8.25	$f_2\rho$	8.45
$\pi(1300)\rho$	7.77	$\eta(1295)\rho$	8.17
$a_2\rho$	5.59	$\rho\rho(1450)$	7.91
$\pi\rho(1450)$	5.32	$b_1\eta$	7.90
$a_0\rho$	4.89	$b_1\rho$	7.84
$h_1\eta(1295)$	4.21	$a_2(1700)\omega$	7.05
$\eta_2\omega$	1.96	$h_1\pi(1300)$	6.56
$f_1(1420)\omega$	1.85	$\pi\pi$	6.40
$\eta\omega$	1.59	$\pi\omega_3$	4.30
f_2h_1	1.59	$\pi\omega$	4.040
$\eta(1295)\omega$	1.55	$a_4(2040)\pi$	3.94
K_1K_1	1.50	$\pi_2\omega$	3.55
$\eta\omega(1420)$	1.50	$\pi(1300)\omega$	2.62
$a_1\rho$	1.37	$a_1\pi(1300)$	2.17
KK_1'	1.34	$f_1(1420)\rho$	1.96
$\eta\omega_3$	1.07	$a_1\omega(1420)$	1.86
$h_1\eta'$	1.01	$b_1\eta(1295)$	1.84
		$a_2\omega$	1.69
		$\eta(1475)\rho$	1.64
		$a_2(1320)h_1$	1.55
		b_1b_1	1.54
		b_1f_1	1.51
		K_1K_1	1.50
		$\eta\rho(1450)$	1.48
		ωa_0	1.48
		$\omega(1420)\pi$	1.43
		h_1a_1	1.39
		$\pi(1300)\pi(1300)$	1.19
		a_2a_2	1.03

In addition, it is our hope and belief that more experimental measurements will be released in the future.

ACKNOWLEDGMENTS

This work is supported by the National Natural Science Foundation of China under Grants No. 11965016 and the Natural Science Foundation of Qinghai Province No. 2020-ZJ-728. Y.-R. W. and T.-Y. L. contributed equally to this work.

[1] M. Ablikim *et al.* (BESIII Collaboration), Phys. Rev. D **105**, 032005 (2022).
[2] Q.-S. Zhou, J.-Z. Wang, and X. Liu, Phys. Rev. D **106**, 034010 (2022).
[3] H. B. Li *et al.* (BESIII Collaboration), arXiv:2204.08943.
[4] C.-Q. Pang, Y.-R. Wang, J.-F. Hu, T.-J. Zhang, and X. Liu, Phys. Rev. D **101**, 074022 (2020).
[5] M. Ablikim *et al.* (BESIII Collaboration), Phys. Rev. D **99**, 032001 (2019).
[6] M. Ablikim *et al.* (BESIII Collaboration), Phys. Lett. B **813**, 136059 (2021).
[7] Z.-Y. Li, D.-M. Li, E. Wang, W.-C. Yan, and Q.-T. Song, Phys. Rev. D **104**, 034013 (2021).
[8] M. Ablikim *et al.* (BESIII Collaboration), Phys. Rev. D **99**, 032001 (2019).
[9] D.-Y. Chen, J. Liu, and J. He, Phys. Rev. D **101**, 074045 (2020).
[10] Q.-F. Lü, K.-L. Wang, and Y.-B. Dong, Chin. Phys. C **44**, 024101 (2020).
[11] K. Azizi, S. S. Agaev, and H. Sundu, Nucl. Phys. **B948**, 114789 (2019).
[12] J.-T. Zhu, Y. Liu, D.-Y. Chen, L. Jiang, and J. He, Chin. Phys. C **44**, 123103 (2020).
[13] S. Afonin, Phys. Rev. C **76**, 015202 (2007).
[14] D. Ebert, R. Faustov, and V. Galkin, Phys. Rev. D **79**, 114029 (2009).
[15] A. V. Anisovich, V. V. Anisovich, L. G. Dakhno, M. A. Matveev, V. A. Nikonov, and A. V. Sarantsev, J. Phys. G **37**, 025004 (2010).
[16] L.-P. He, X. Wang, and X. Liu, Phys. Rev. D **88**, 034008 (2013).
[17] L.-M. Wang, S.-Q. Luo, and X. Liu, Phys. Rev. D **105**, 034011 (2022).
[18] J.-C. Feng, X.-W. Kang, Q.-F. Lü, and F.-S. Zhang, Phys. Rev. D **104**, 054027 (2021).
[19] X.-C. Feng, Z.-Y. Li, D.-M. Li, Q.-T. Song, E. Wang, and W.-C. Yan, arXiv:2206.10132.
[20] C. T. Johnson and J. J. Dudek (Hadron Spectrum Collaboration), Phys. Rev. D **103**, 074502 (2021).
[21] G. F. Chew and S. C. Frautschi, Phys. Rev. Lett. **8**, 41 (1962).
[22] A. Anisovich, V. Anisovich, and A. Sarantsev, Phys. Rev. D **62**, 051502 (2000).
[23] S. Godfrey and N. Isgur, Phys. Rev. D **32**, 189 (1985).
[24] Q.-T. Song, D.-Y. Chen, X. Liu, and T. Matsuki, Phys. Rev. D **91**, 054031 (2015).
[25] Q.-T. Song, D.-Y. Chen, X. Liu, and T. Matsuki, Phys. Rev. D **92**, 074011 (2015).
[26] W. Lucha, F. F. Schoberl, and D. Gromes, Phys. Rep. **200**, 127 (1991).
[27] C.-Q. Pang, Y.-R. Wang, and C.-H. Wang, Phys. Rev. D **99**, 014022 (2019).
[28] L. Micu, Nucl. Phys. **B10**, 521 (1969).
[29] A. Le Yaouanc, L. Oliver, O. Pene, and J. Raynal, Phys. Rev. D **8**, 2223 (1973).
[30] A. Le Yaouanc, L. Oliver, O. Pene, and J.-C. Raynal, Phys. Rev. D **9**, 1415 (1974).
[31] A. Le Yaouanc, L. Oliver, O. Pene, and J. Raynal, Phys. Rev. D **11**, 1272 (1975).
[32] A. Le Yaouanc, L. Oliver, O. Pene, and J. Raynal, Phys. Lett. **72B**, 57 (1977).
[33] A. Le Yaouanc, L. Oliver, O. Pene, and J.-C. Raynal, Phys. Lett. **71B**, 397 (1977).
[34] E. van Beveren, C. Dullemond, and G. Rupp, Phys. Rev. D **21**, 772 (1980); **22**, 787(E) (1980).
[35] E. van Beveren, G. Rupp, T. Rijken, and C. Dullemond, Phys. Rev. D **27**, 1527 (1983).
[36] S. Capstick and W. Roberts, Phys. Rev. D **49**, 4570 (1994).
[37] P. R. Page, Nucl. Phys. **B446**, 189 (1995).
[38] A. I. Titov, T. I. Gulamov, and B. Kampfer, Phys. Rev. D **53**, 3770 (1996).
[39] E. Ackleh, T. Barnes, and E. Swanson, Phys. Rev. D **54**, 6811 (1996).
[40] H. G. Blundell, arXiv:hep-ph/9608473.
[41] R. Bonnaz, B. Silvestre-Brac, and C. Gignoux, Eur. Phys. J. A **13**, 363 (2002).
[42] H. Q. Zhou, R. G. Ping, and B. S. Zou, Phys. Lett. B **611**, 123 (2005).
[43] J. Lu, X.-L. Chen, W.-Z. Deng, and S.-L. Zhu, Phys. Rev. D **73**, 054012 (2006).
[44] B. Zhang, X. Liu, W.-Z. Deng, and S.-L. Zhu, Eur. Phys. J. C **50**, 617 (2007).
[45] Z.-G. Luo, X.-L. Chen, and X. Liu, Phys. Rev. D **79**, 074020 (2009).
[46] Z.-F. Sun and X. Liu, Phys. Rev. D **80**, 074037 (2009).
[47] X. Liu, Z.-G. Luo, and Z.-F. Sun, Phys. Rev. Lett. **104**, 122001 (2010).
[48] Z.-F. Sun, J.-S. Yu, X. Liu, and T. Matsuki, Phys. Rev. D **82**, 111501 (2010).
[49] T. Rijken, M. Nagels, and Y. Yamamoto, Nucl. Phys. **A835**, 160 (2010).
[50] Z.-C. Ye, X. Wang, X. Liu, and Q. Zhao, Phys. Rev. D **86**, 054025 (2012).
[51] X. Wang, Z.-F. Sun, D.-Y. Chen, X. Liu, and T. Matsuki, Phys. Rev. D **85**, 074024 (2012).
[52] Y. Sun, X. Liu, and T. Matsuki, Phys. Rev. D **88**, 094020 (2013).
[53] C.-Q. Pang, L.-P. He, X. Liu, and T. Matsuki, Phys. Rev. D **90**, 014001 (2014).
[54] B. Wang, C.-Q. Pang, X. Liu, and T. Matsuki, Phys. Rev. D **91**, 014025 (2015).
[55] K. Chen, C.-Q. Pang, X. Liu, and T. Matsuki, Phys. Rev. D **91**, 074025 (2015).
[56] C.-Q. Pang, J.-Z. Wang, X. Liu, and T. Matsuki, Eur. Phys. J. C **77**, 861 (2017).
[57] M. Jacob and G. Wick, Ann. Phys. (N.Y.) **7**, 404 (1959).
[58] D. Jia, C.-Q. Pang, and A. Hosaka, Int. J. Mod. Phys. A **32**, 1750153 (2017).
[59] V. V. Anisovich, L. G. Dakhno, M. A. Matveev, V. A. Nikonov, and A. V. Sarantsev, Phys. At. Nucl. **70**, 450 (2007).
[60] P. A. Zyla *et al.* (Particle Data Group), Prog. Theor. Exp. Phys. **2020**, 083C01 (2020).
[61] B. Aubert, M. Bona, D. Boutigny, Y. Karyotakis, J. Lees, V. Poireau, X. Prudent, V. Tisserand, A. Zghiche, J. G. Tico *et al.*, Phys. Rev. D **77**, 092002 (2008).
[62] J. P. Lees, V. Poireau, and V. Tisserand (*BABAR* Collaboration), Phys. Rev. D **101**, 012011 (2020).
[63] D. V. Bugg, Phys. Rep. **397**, 257 (2004).
[64] F. Buisseret and C. Semay, Phys. Rev. D **71**, 034019 (2005).
[65] C.-Q. Pang, B. Wang, X. Liu, and T. Matsuki, Phys. Rev. D **92**, 014012 (2015).

[66] M. Tanabashi *et al.* (Particle Data Group), Phys. Rev. D **98**, 030001 (2018).
[67] T. Barnes, F. Close, P. Page, and E. Swanson, Phys. Rev. D **55**, 4157 (1997).
[68] V. M. Aul'chenko *et al.*J. Exp. Theor. Phys. **121**, 27 (2015).
[69] A. Anisovich, C. Baker, C. Batty, D. Bugg, L. Montanet, V. A. Nikonov, A. V. Sarantsev, V. V. Sarantsev, and B. S. Zou, Phys. Lett. B **542**, 19 (2002).
[70] P. A. Zyla *et al.* (Particle Data Group), Prog. Theor. Exp. Phys. **2020**, 083C01 (2020).
[71] D. Bugg, Eur. Phys. J. C **36**, 161 (2004).
[72] B. Aubert *et al.* (*BABAR* Collaboration),Phys. Rev. D **76**, 092005 (2007); **77**, 119902(E) (2008).
[73] L.-M. Wang, J.-Z. Wang, and X. Liu, Phys. Rev. D **102**, 034037 (2020).
[74] T. Collaboration and A. Abele, Eur. Phys. J. C **21**, 261 (2001).
[75] K. Kittimanapun, K. Khosonthongkee, C. Kobdaj, P. Suebka, and Y. Yan, Phys. Rev. C **79**, 025201 (2009).
[76] A. Hasan and D. Bugg, Phys. Lett. B **334**, 215 (1994).
[77] A. V. Anisovich, C. A. Baker, C. J. Batty, D. V. Bugg, C. Hodd, H. C Lu, V. A. Nikonov, A. V. Sarantsev, V. V Sarantsev, and B. S. Zou, Phys. Lett. B **491**, 47 (2000).
[78] D. V. Amelin, E. B. Berdnikov, S. I. Bityukov, G. V. Borisov, V. A. Dorofeev, R. I. Dzhelyadin, Y. P. Gouz, I. A. Kachaev, K. Y. A. Khokhlov, and E. Al, Z. Phys. C **70**, 71 (1996).
[79] C. Baltay, C. V. Cautis, and M. V. Kalelkar, Phys. Rev. Lett. **40**, 87 (1978).
[80] V. E. Barnes, S. U. Chung, R. L. Eisner, E. Flaminio, P. Guidoni, J. B. Kinson, and N. P. Samios, Phys. Rev. Lett. **23**, 142 (1969).
[81] A. V. Anisovich, C. A. Baker, C. J. Batty, D. V. Bugg, L. Montanet, V. A. Nikonov, A. V. Sarantsev, V. V. Sarantsev, and B. S. Zou, Phys. Lett. B **542**, 19 (2002).
[82] M. Coupland, E. Eisenhandler, W. R. Gibson, P. Kalmus, and A. Astbury, Phys. Lett. B **71**, 460 (1977).